Fermilab FERMILAB-PUB-05-337-E CDF

Search for New High Mass Particles Decaying to Lepton Pairs in $p\bar{p}$ Collisions at $\sqrt{s} = 1.96$ TeV

A. Abulencia,[23] D. Acosta,[17] J. Adelman,[13] T. Affolder,[10] T. Akimoto,[53] M.G. Albrow,[16] D. Ambrose,[16] S. Amerio,[42] D. Amidei,[33] A. Anastassov,[50] K. Anikeev,[16] A. Annovi,[44] J. Antos,[1] M. Aoki,[53] G. Apollinari,[16] J.-F. Arguin,[32] T. Arisawa,[55] A. Artikov,[14] W. Ashmanskas,[16] A. Attal,[8] F. Azfar,[41] P. Azzi-Bacchetta,[42] P. Azzurri,[44] N. Bacchetta,[42] H. Bachacou,[28] W. Badgett,[16] A. Barbaro-Galtieri,[28] V.E. Barnes,[46] B.A. Barnett,[24] S. Baroiant,[7] V. Bartsch,[30] G. Bauer,[31] F. Bedeschi,[44] S. Behari,[24] S. Belforte,[52] G. Bellettini,[44] J. Bellinger,[57] A. Belloni,[31] E. Ben-Haim,[16] D. Benjamin,[15] A. Beretvas,[16] J. Beringer,[28] T. Berry,[29] A. Bhatti,[48] M. Binkley,[16] D. Bisello,[42] M. Bishai,[16] R. E. Blair,[2] C. Blocker,[6] K. Bloom,[33] B. Blumenfeld,[24] A. Bocci,[48] A. Bodek,[47] V. Boisvert,[47] G. Bolla,[46] A. Bolshov,[31] D. Bortoletto,[46] J. Boudreau,[45] S. Bourov,[16] A. Boveia,[10] B. Brau,[10] C. Bromberg,[34] E. Brubaker,[13] J. Budagov,[14] H.S. Budd,[47] S. Budd,[23] K. Burkett,[16] G. Busetto,[42] P. Bussey,[20] K. L. Byrum,[2] S. Cabrera,[15] M. Campanelli,[19] M. Campbell,[33] F. Canelli,[8] A. Canepa,[46] D. Carlsmith,[57] R. Carosi,[44] S. Carron,[15] M. Casarsa,[52] A. Castro,[5] P. Catastini,[44] D. Cauz,[52] M. Cavalli-Sforza,[3] A. Cerri,[28] L. Cerrito,[41] S.H. Chang,[27] J. Chapman,[33] Y.C. Chen,[1] M. Chertok,[7] G. Chiarelli,[44] G. Chlachidze,[14] F. Chlebana,[16] I. Cho,[27] K. Cho,[27] D. Chokheli,[14] J.P. Chou,[21] P.H. Chu,[23] S.H. Chuang,[57] K. Chung,[12] W.H. Chung,[57] Y.S. Chung,[47] M. Ciljak,[44] C.I. Ciobanu,[23] M.A. Ciocci,[44] A. Clark,[19] D. Clark,[6] M. Coca,[15] A. Connolly,[28] M. E. Convery,[48] J. Conway,[7] B. Cooper,[30] K. Copic,[33] M. Cordelli,[18] G. Cortiana,[42] A. Cruz,[17] J. Cuevas,[11] R. Culbertson,[16] D. Cyr,[57] S. DaRonco,[42] S. D'Auria,[20] M. D'onofrio,[19] D. Dagenhart,[6] P. de Barbaro,[47] S. De Cecco,[49] A. Deisher,[28] G. De Lentdecker,[47] M. Dell'Orso,[44] S. Demers,[47] L. Demortier,[48] J. Deng,[15] M. Deninno,[5] D. De Pedis,[49] P.F. Derwent,[16] C. Dionisi,[49] J. Dittmann,[4] P. DiTuro,[50] C. Dörr,[25] A. Dominguez,[28] S. Donati,[44] M. Donega,[19] P. Dong,[8] J. Donini,[42] T. Dorigo,[42] S. Dube,[50] K. Ebina,[55] J. Efron,[38] J. Ehlers,[19] R. Erbacher,[7] D. Errede,[23] S. Errede,[23] R. Eusebi,[47] H.C. Fang,[28] S. Farrington,[29] I. Fedorko,[44] W.T. Fedorko,[13] R.G. Feild,[58] M. Feindt,[25] J.P. Fernandez,[46] R. Field,[17] G. Flanagan,[34] L.R. Flores-Castillo,[45] A. Foland,[21] S. Forrester,[7] G.W. Foster,[16] M. Franklin,[21] J.C. Freeman,[28] Y. Fujii,[26] I. Furic,[13] A. Gajjar,[29] M. Gallinaro,[48] J. Galyardt,[12] J.E. Garcia,[44] M. Garcia Sciverez,[28] A.F. Garfinkel,[46] C. Gay,[58] H. Gerberich,[23] E. Gerchtein,[12] D. Gerdes,[33] S. Giagu,[49] P. Giannetti,[44] A. Gibson,[28] K. Gibson,[12] C. Ginsburg,[16] K. Giolo,[46] M. Giordani,[52] M. Giunta,[44] G. Giurgiu,[12] V. Glagolev,[14] D. Glenzinski,[16] M. Gold,[36] N. Goldschmidt,[33] J. Goldstein,[41] G. Gomez,[11] G. Gomez-Ceballos,[11] M. Goncharov,[51] O. González,[46] I. Gorelov,[36] A.T. Goshaw,[15] Y. Gotra,[45] K. Goulianos,[48] A. Gresele,[42] M. Griffiths,[29] S. Grinstein,[21] C. Grosso-Pilcher,[13] U. Grundler,[23] J. Guimaraes da Costa,[21] C. Haber,[28] S.R. Hahn,[16] K. Hahn,[43] E. Halkiadakis,[47] A. Hamilton,[32] B-Y. Han,[47] R. Handler,[57] F. Happacher,[18] K. Hara,[53] M. Hare,[54] S. Harper,[41] R.F. Harr,[56] R.M. Harris,[16] K. Hatakeyama,[48] J. Hauser,[8] C. Hays,[15] H. Hayward,[29] A. Heijboer,[43] B. Heinemann,[29] J. Heinrich,[43] M. Hennecke,[25] M. Herndon,[57] J. Heuser,[25] D. Hidas,[15] C.S. Hill,[10] D. Hirschbuehl,[25] A. Hocker,[16] A. Holloway,[21] S. Hou,[1] M. Houlden,[29] S.-C. Hsu,[9] B.T. Huffman,[41] R.E. Hughes,[38] J. Huston,[34] K. Ikado,[55] J. Incandela,[10] G. Introzzi,[44] M. Iori,[49] Y. Ishizawa,[53] A. Ivanov,[7] B. Iyutin,[31] E. James,[16] D. Jang,[50] B. Jayatilaka,[33] D. Jeans,[49] H. Jensen,[16] E.J. Jeon,[27] M. Jones,[46] K.K. Joo,[27] S.Y. Jun,[12] T.R. Junk,[23] T. Kamon,[51] J. Kang,[33] M. Karagoz-Unel,[37] P.E. Karchin,[56] Y. Kato,[40] Y. Kemp,[25] R. Kephart,[16] U. Kerzel,[25] V. Khotilovich,[51] B. Kilminster,[38] D.H. Kim,[27] H.S. Kim,[27] J.E. Kim,[27] M.J. Kim,[12] M.S. Kim,[27] S.B. Kim,[27] S.H. Kim,[53] Y.K. Kim,[13] M. Kirby,[15] L. Kirsch,[6] S. Klimenko,[17] M. Klute,[31] B. Knuteson,[31] B.R. Ko,[15] H. Kobayashi,[53] K. Kondo,[55] D.J. Kong,[27] J. Konigsberg,[17] A. Korytov,[17] A.V. Kotwal,[15] A. Kovalev,[43] J. Kraus,[23] I. Kravchenko,[31] M. Kreps,[25] A. Kreymer,[16] J. Kroll,[43] N. Krumnack,[4] M. Kruse,[15] V. Krutelyov,[51] S. E. Kuhlmann,[2] Y. Kusakabe,[55] S. Kwang,[13] A.T. Laasanen,[46] S. Lai,[32] S. Lami,[48] S. Lami,[48] S. Lammel,[16] M. Lancaster,[30] R. L. Lander,[7] K. Lannon,[38] A. Lath,[50] G. Latino,[44] I. Lazzizzera,[42] C. Lecci,[25] T. LeCompte,[2] J. Lee,[47] J. Lee,[47] S.W. Lee,[51] R. Lefèvre,[3] N. Leonardo,[31] S. Leone,[44] S. Levy,[13] J.D. Lewis,[16] K. Li,[58] C. Lin,[58] C.S. Lin,[16] M. Lindgren,[16] E. Lipeles,[9] T.M. Liss,[23] A. Lister,[19] D.O. Litvintsev,[16] T. Liu,[16] Y. Liu,[19] N.S. Lockyer,[43] A.Loginov,[35] M. Loreti,[42] P. Loverre,[49] R.-S. Lu,[1] D. Lucchesi,[42] P. Lujan,[28] P. Lukens,[16] G. Lungu,[17] L. Lyons,[41] J. Lys,[28] R. Lysak,[1] E. Lytken,[46] P. Mack,[25] D. MacQueen,[32] R. Madrak,[16] K. Maeshima,[16] P. Maksimovic,[24] G. Manca,[29] F. Margaroli,[5] R. Marginean,[16] C. Marino,[23] A. Martin,[58] M. Martin,[24] V. Martin,[37] M. Martínez,[3] T. Maruyama,[53] H. Matsunaga,[53] M.E. Mattson,[56] R. Mazini,[32] P. Mazzanti,[5] K.S. McFarland,[47] D. McGivern,[30] P. McIntyre,[51] P. McNamara,[50] R. McNulty,[29] A. Mehta,[29] S. Menzemer,[31] A. Menzione,[44] P. Merkel,[46] C. Mesropian,[48] A. Messina,[49]

M. von der Mey,[8] T. Miao,[16] N. Miladinovic,[6] J. Miles,[31] R. Miller,[34] J.S. Miller,[33] C. Mills,[10] M. Milnik,[25] R. Miquel,[28] S. Miscetti,[18] G. Mitselmakher,[17] A. Miyamoto,[26] N. Moggi,[5] B. Mohr,[8] R. Moore,[16] M. Morello,[44] P. Movilla Fernandez,[28] J. Mülmenstädt,[28] A. Mukherjee,[16] M. Mulhearn,[31] Th. Muller,[25] R. Mumford,[24] P. Murat,[16] J. Nachtman,[16] S. Nahn,[58] I. Nakano,[39] A. Napier,[54] D. Naumov,[36] V. Necula,[17] C. Neu,[43] M.S. Neubauer,[9] J. Nielsen,[28] T. Nigmanov,[45] L. Nodulman,[2] O. Norniella,[3] T. Ogawa,[55] S.H. Oh,[15] Y.D. Oh,[27] T. Okusawa,[40] R. Oldeman,[29] R. Orava,[22] K. Osterberg,[22] C. Pagliarone,[44] E. Palencia,[11] R. Paoletti,[44] V. Papadimitriou,[16] A. Papikonomou,[25] A.A. Paramonov,[13] B. Parks,[38] S. Pashapour,[32] J. Patrick,[16] G. Pauletta,[52] M. Paulini,[12] C. Paus,[31] D. E. Pellett,[7] A. Penzo,[52] T.J. Phillips,[15] G. Piacentino,[44] J. Piedra,[11] K. Pitts,[23] C. Plager,[8] L. Pondrom,[57] G. Pope,[45] X. Portell,[3] O. Poukhov,[14] N. Pounder,[41] F. Prakoshyn,[14] A. Pronko,[16] J. Proudfoot,[2] F. Ptohos,[18] G. Punzi,[44] J. Pursley,[24] J. Rademacker,[41] A. Rahaman,[45] A. Rakitin,[31] S. Rappoccio,[21] F. Ratnikov,[50] B. Reisert,[16] V. Rekovic,[36] N. van Remortel,[22] P. Renton,[41] M. Rescigno,[49] S. Richter,[25] F. Rimondi,[5] K. Rinnert,[25] L. Ristori,[44] W.J. Robertson,[15] A. Robson,[20] T. Rodrigo,[11] E. Rogers,[23] S. Rolli,[54] R. Roser,[16] M. Rossi,[52] R. Rossin,[17] C. Rott,[46] A. Ruiz,[11] J. Russ,[12] V. Rusu,[13] D. Ryan,[54] H. Saarikko,[22] S. Sabik,[32] A. Safonov,[7] W.K. Sakumoto,[47] G. Salamanna,[49] O. Salto,[3] D. Saltzberg,[8] C. Sanchez,[3] L. Santi,[52] S. Sarkar,[49] K. Sato,[53] P. Savard,[32] A. Savoy-Navarro,[16] T. Scheidle,[25] P. Schlabach,[16] E.E. Schmidt,[16] M.P. Schmidt,[58] M. Schmitt,[37] T. Schwarz,[33] L. Scodellaro,[11] A.L. Scott,[10] A. Scribano,[44] F. Scuri,[44] A. Sedov,[46] S. Seidel,[36] Y. Seiya,[40] A. Semenov,[14] F. Semeria,[5] L. Sexton-Kennedy,[16] I. Sfiligoi,[18] M.D. Shapiro,[28] T. Shears,[29] P.F. Shepard,[45] D. Sherman,[21] M. Shimojima,[53] M. Shochet,[13] Y. Shon,[57] I.Shreyber,[35] A. Sidoti,[44] P. Sinervo,[32] A. Sisakyan,[14] J. Sjolin,[41] A. Skiba,[25] A.J. Slaughter,[16] K. Sliwa,[54] D. Smirnov,[36] J. R. Smith,[7] F.D. Snider,[16] R. Snihur,[32] M. Soderberg,[33] A. Soha,[7] S. Somalwar,[50] V. Sorin,[34] J. Spalding,[16] F. Spinella,[44] P. Squillacioti,[44] M. Stanitzki,[58] A. Staveris-Polykalas,[44] R. St. Denis,[20] B. Stelzer,[8] O. Stelzer-Chilton,[32] D. Stentz,[37] J. Strologas,[36] D. Stuart,[10] J.S. Suh,[27] A. Sukhanov,[17] K. Sumorok,[31] H. Sun,[54] T. Suzuki,[53] A. Taffard,[23] R. Tafirout,[32] R. Takashima,[39] Y. Takeuchi,[53] K. Takikawa,[53] M. Tanaka,[2] R. Tanaka,[39] M. Tecchio,[33] P.K. Teng,[1] K. Terashi,[48] S. Tether,[31] J. Thom,[16] A.S. Thompson,[20] E. Thomson,[43] P. Tipton,[47] V. Tiwari,[12] S. Tkaczyk,[16] D. Toback,[51] K. Tollefson,[34] T. Tomura,[53] D. Tonelli,[44] M. Tönnesmann,[34] S. Torre,[44] D. Torretta,[16] S. Tourneur,[16] W. Trischuk,[32] R. Tsuchiya,[55] S. Tsuno,[39] N. Turini,[44] F. Ukegawa,[53] T. Unverhau,[20] S. Uozumi,[53] D. Usynin,[43] L. Vacavant,[28] A. Vaiciulis,[47] S. Vallecorsa,[19] A. Varganov,[33] E. Vataga,[36] G. Velev,[16] G. Veramendi,[23] V. Veszpremi,[46] T. Vickey,[23] R. Vidal,[16] I. Vila,[11] R. Vilar,[11] I. Vollrath,[32] I. Volobouev,[28] F. Würthwein,[9] P. Wagner,[51] R. G. Wagner,[2] R.L. Wagner,[16] W. Wagner,[25] R. Wallny,[8] T. Walter,[25] Z. Wan,[50] M.J. Wang,[1] S.M. Wang,[17] A. Warburton,[32] B. Ward,[20] S. Waschke,[20] D. Waters,[30] T. Watts,[50] M. Weber,[28] W.C. Wester III,[16] B. Whitehouse,[54] D. Whiteson,[43] A. B. Wicklund,[2] E. Wicklund,[16] H.H. Williams,[43] P. Wilson,[16] B.L. Winer,[38] P. Wittich,[43] S. Wolbers,[16] C. Wolfe,[13] S. Worm,[50] T. Wright,[33] X. Wu,[19] S.M. Wynne,[29] A. Yagil,[16] K. Yamamoto,[40] J. Yamaoka,[50] Y. Yamashita.,[39] C. Yang,[58] U.K. Yang,[13] W.M. Yao,[28] G.P. Yeh,[16] J. Yoh,[16] K. Yorita,[13] T. Yoshida,[40] I. Yu,[27] S.S. Yu,[43] J.C. Yun,[16] L. Zanello,[49] A. Zanetti,[52] I. Zaw,[21] F. Zetti,[44] X. Zhang,[23] J. Zhou,[50] and S. Zucchelli[5]

(CDF Collaboration)

[1]*Institute of Physics, Academia Sinica, Taipei, Taiwan 11529, Republic of China*
[2]*Argonne National Laboratory, Argonne, Illinois 60439*
[3]*Institut de Fisica d'Altes Energies, Universitat Autonoma de Barcelona, E-08193, Bellaterra (Barcelona), Spain*
[4]*Baylor University, Waco, Texas 76798*
[5]*Istituto Nazionale di Fisica Nucleare, University of Bologna, I-40127 Bologna, Italy*
[6]*Brandeis University, Waltham, Massachusetts 02254*
[7]*University of California, Davis, Davis, California 95616*
[8]*University of California, Los Angeles, Los Angeles, California 90024*
[9]*University of California, San Diego, La Jolla, California 92093*
[10]*University of California, Santa Barbara, Santa Barbara, California 93106*
[11]*Instituto de Fisica de Cantabria, CSIC-University of Cantabria, 39005 Santander, Spain*
[12]*Carnegie Mellon University, Pittsburgh, PA 15213*
[13]*Enrico Fermi Institute, University of Chicago, Chicago, Illinois 60637*
[14]*Joint Institute for Nuclear Research, RU-141980 Dubna, Russia*
[15]*Duke University, Durham, North Carolina 27708*
[16]*Fermi National Accelerator Laboratory, Batavia, Illinois 60510*
[17]*University of Florida, Gainesville, Florida 32611*
[18]*Laboratori Nazionali di Frascati, Istituto Nazionale di Fisica Nucleare, I-00044 Frascati, Italy*
[19]*University of Geneva, CH-1211 Geneva 4, Switzerland*

[20] Glasgow University, Glasgow G12 8QQ, United Kingdom
[21] Harvard University, Cambridge, Massachusetts 02138
[22] Division of High Energy Physics, Department of Physics, University of Helsinki and Helsinki Institute of Physics, FIN-00014, Helsinki, Finland
[23] University of Illinois, Urbana, Illinois 61801
[24] The Johns Hopkins University, Baltimore, Maryland 21218
[25] Institut für Experimentelle Kernphysik, Universität Karlsruhe, 76128 Karlsruhe, Germany
[26] High Energy Accelerator Research Organization (KEK), Tsukuba, Ibaraki 305, Japan
[27] Center for High Energy Physics: Kyungpook National University, Taegu 702-701; Seoul National University, Seoul 151-742; and SungKyunKwan University, Suwon 440-746; Korea
[28] Ernest Orlando Lawrence Berkeley National Laboratory, Berkeley, California 94720
[29] University of Liverpool, Liverpool L69 7ZE, United Kingdom
[30] University College London, London WC1E 6BT, United Kingdom
[31] Massachusetts Institute of Technology, Cambridge, Massachusetts 02139
[32] Institute of Particle Physics: McGill University, Montréal, Canada H3A 2T8; and University of Toronto, Toronto, Canada M5S 1A7
[33] University of Michigan, Ann Arbor, Michigan 48109
[34] Michigan State University, East Lansing, Michigan 48824
[35] Institution for Theoretical and Experimental Physics, ITEP, Moscow 117259, Russia
[36] University of New Mexico, Albuquerque, New Mexico 87131
[37] Northwestern University, Evanston, Illinois 60208
[38] The Ohio State University, Columbus, Ohio 43210
[39] Okayama University, Okayama 700-8530, Japan
[40] Osaka City University, Osaka 588, Japan
[41] University of Oxford, Oxford OX1 3RH, United Kingdom
[42] University of Padova, Istituto Nazionale di Fisica Nucleare, Sezione di Padova-Trento, I-35131 Padova, Italy
[43] University of Pennsylvania, Philadelphia, Pennsylvania 19104
[44] Istituto Nazionale di Fisica Nucleare Pisa, Universities of Pisa, Siena and Scuola Normale Superiore, I-56127 Pisa, Italy
[45] University of Pittsburgh, Pittsburgh, Pennsylvania 15260
[46] Purdue University, West Lafayette, Indiana 47907
[47] University of Rochester, Rochester, New York 14627
[48] The Rockefeller University, New York, New York 10021
[49] Istituto Nazionale di Fisica Nucleare, Sezione di Roma 1, University di Roma "La Sapienza," I-00185 Roma, Italy
[50] Rutgers University, Piscataway, New Jersey 08855
[51] Texas A&M University, College Station, Texas 77843
[52] Istituto Nazionale di Fisica Nucleare, University of Trieste/ Udine, Italy
[53] University of Tsukuba, Tsukuba, Ibaraki 305, Japan
[54] Tufts University, Medford, Massachusetts 02155
[55] Waseda University, Tokyo 169, Japan
[56] Wayne State University, Detroit, Michigan 48201
[57] University of Wisconsin, Madison, Wisconsin 53706
[58] Yale University, New Haven, Connecticut 06520

(Dated: July 25, 2005)

A search for new particles (X) that decay to electron or muon pairs has been performed using approximately 200 pb^{-1} of $p\bar{p}$ collision data at $\sqrt{s} = 1.96$ TeV collected by the CDF II experiment at the Fermilab Tevatron. Limits on $\sigma(p\bar{p} \to X) \cdot BR(X \to \ell\ell)$ are presented as a function of dilepton invariant mass $m_{\ell\ell} > 150$ GeV/c^2, for different spin hypotheses (0, 1, or 2). The limits are approximately 25 fb for $m_{\ell\ell} > 600$ GeV/c^2. Lower mass bounds for X from representative models beyond the Standard Model including heavy neutral gauge bosons are presented.

PACS numbers: 13.85.Rm, 12.38.Qk, 13.85.Qk, 14.70.Pw, 12.60.Cn

A search for new particles (X) has been performed in the dilepton (ee and $\mu\mu$) decay channel using $p\bar{p}$ collision data at $\sqrt{s} = 1.96$ TeV collected by the upgraded Collider Detector at Fermilab (CDF II) at the Tevatron. The observed dilepton invariant mass ($m_{\ell\ell}$) distribution is compared with that expected from Standard Model (SM) processes for $m_{\ell\ell} > 150$ GeV/c^2. Many models beyond the SM predict such particles with masses at or below the TeV scale [1]. Generic searches for spin-0, 1, and 2 particles are performed, taking into account the dependence of the experimental acceptance on the spin-dependent angular distributions of the lepton pair. While this approach provides sensitivity to broad classes of new models, the spin-1 result addresses an issue of fundamental importance in particle physics: the possible existence of extra neutral gauge bosons expected in many models with a higher gauge structure than that of the SM. A generic SM-like (sequential) Z' boson ($Z'_{\rm SM}$) is defined to have the same coupling strengths to fermions as those of the SM Z^0 boson and its mass bound provides a convenient reference indicating the experimental sensitivity. The previous best $Z'_{\rm SM}$ lower mass bounds from direct searches are 690 GeV/c^2 by the CDF collaboration [2] and 670 GeV/c^2 by the D0 collaboration [3] at the 95% confidence level (CL) [4]. Increased integrated luminosity and center-of-mass energy for Run II are expected to provide a significant improvement over these previous results. Indirect limits on the mass of Z' bosons have been set by the LEP II experiments [5]. A more detailed discussion of the LEP results and the advantages of the Tevatron search can be found in Reference [6]. In addition to $Z'_{\rm SM}$, we consider Z' bosons (spin-1) from the E_6 model (Z_χ, Z_ψ, Z_η, Z_I) [7] and the Littlest Higgs model (Z_H) [8], Technicolor (TC) particles (spin-1) [9], sneutrinos ($\widetilde{\nu}$) in an R-parity violating supersymmetric (RPV SUSY) model (spin-0) [10], and gravitons in the Randall-Sundrum (RS) warped extra dimension model (spin-2) [11]. Independent of specific models, the limits on $\sigma(X_{\ell\ell}) \equiv \sigma(p\bar{p} \to X) \cdot BR(X \to \ell\ell)$ presented here can be used to set lower bounds on the mass of X (m_X) in many classes of models with a narrow width resonance. Using the spin-1 $\sigma(X_{\ell\ell})$ limit result, bounds on the couplings in more generalized Z' models [6] have been derived and are presented.

The CDF II detector is a forward-backward and azimuthally symmetric detector with a tracking system immersed in a 1.4 T solenoidal magnetic field, calorimetry for measuring the energies of particles, and detectors to identify deeply-penetrating muons [12]. The tracking system consists of an open-cell drift chamber, the Central Outer Tracker (COT), surrounding an eight layer silicon tracker. The fiducial coverage of the COT is $|\eta| < 1.0$ and the silicon extends this coverage forward to $|\eta| < 1.8$ [13]. The tracking system is surrounded by electromagnetic (EM) and hadronic (HAD) calorimeters that are divided into a central calorimeter ($|\eta| < 1.1$) and two forward, or "plug", calorimeters ($1.2 < |\eta| < 3.6$). Drift chambers, located outside the hadronic calorimeters and also outside an additional 60 cm of iron shield, detect muons having $|\eta| < 1.0$.

Candidate events are selected from data collected during 2002 - 2003, corresponding to an integrated luminosity ranging from 173 to 200 pb^{-1}, depending upon the detector elements required for the analysis. Dielectron events with a central candidate are collected using a single-electron trigger requiring a loosely-selected electron in the central EM calorimeter (CEM) with $E_{\rm T} >$ 18 GeV and a matching COT track with $p_{\rm T} > 9$ GeV/c. Dielectron events without a central candidate are collected using a trigger requiring two loosely-selected electron candidates in the plug EM calorimeter (PEM) with $E_{\rm T} > 18$ GeV and no tracking requirement. Additional triggers with higher $E_{\rm T}$ thresholds but looser electron-selection requirements are used to ensure full efficiency for high-mass events. Together, these triggers are essentially 100% efficient for the ee decay mode for $m_{\ell\ell} > 150$ GeV/c^2. Dimuon candidate events are collected with single-muon triggers which require a muon chamber track with a matching track measured by the COT with $p_{\rm T} > 18$ GeV/c. The overall trigger efficiency for the $\mu\mu$ decay mode is above 90%.

The dilepton event selection requires at least two electron or two muon candidates with no charge requirement. Both electron and muon candidates are required to be isolated with a cut on the energy found within a cone of angular radius $R = \sqrt{(\delta\phi)^2 + (\delta\eta)^2} = 0.4$ around the lepton candidate. Electron candidates require an EM cluster with $E_{\rm T} > 25$ GeV and longitudinal and transverse shower profiles consistent with electrons [14]. At least one of the two electrons is required to have a matching track, except for events with two central electrons, which both require matching tracks. The inclusion of events with two forward electrons is possible due to a calorimeter-seeded forward tracking algorithm [15]. Events with a significant amount of $\not\!\!E_T$are rejected to remove W+jets and others backgrounds with unreconstructed particles. All muon candidates are required to have a COT track with $p_{\rm T} > 20$ GeV/c and calorimeter energy deposition consistent with a minimum-ionizing particle signal, where at least one candidate must also have a matching track in the muon chambers. To reject cosmic-ray events, muon candidates are required to have COT hit-timing consistent with outward-moving particles [16].

The selected data contains 14,799 ee and 7,775 $\mu\mu$ candidate events with the dilepton invariant mass distributions shown in Fig. 1. These samples are dominated by events in the Z^0 peak. In this region the dielectron sample has a larger acceptance; however, in the high-mass search region the two channels have similar sensitivity. The lepton identification efficiencies are estimated using a purified sample of dilepton events from Z^0 decays [2]. Since leptons from the decay of high-mass objects typically have higher $p_{\rm T}$ than this sample, the lepton identification efficiency is studied as a function of $p_{\rm T}$, and the selection criteria are chosen to ensure high efficiencies throughout the relevant $p_{\rm T}$ range [17, 18]. The geometric and kinematic acceptance as a function of resonance mass is estimated using Monte Carlo (MC) samples: the PYTHIA event generator [19] with CTEQ5L parton distribution functions (PDF) [20] and the CDF II detector simulation are used except as noted. Signal samples for the heavy Higgs (spin-0), $Z'_{\rm SM}$ (spin-1) and RS Graviton (spin-2) are generated to model each spin hypothe-

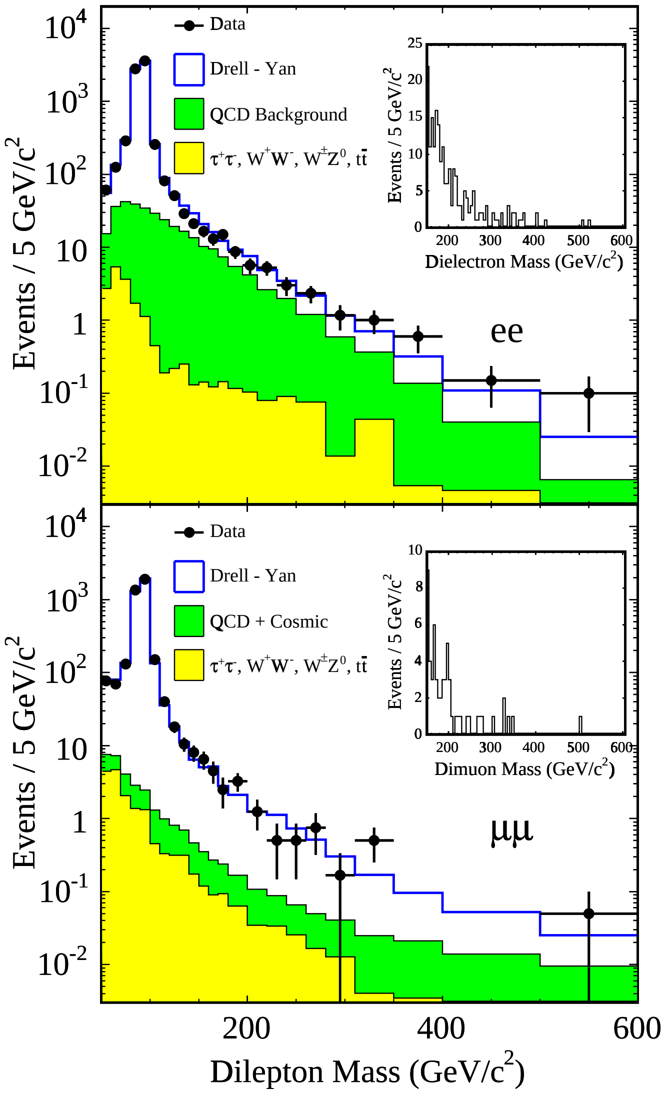

FIG. 1: The ee (top) and $\mu\mu$ (bottom) invariant mass distributions of the observed data (points) with the background prediction (solid line). The background is corrected for acceptance and efficiency. The insets show the data with a fixed bin width of 5 GeV/c^2 for $m_{\ell\ell} > 150$ GeV/c^2.

sis. The product of acceptance and selection efficiency is approximately 50% for $m_X > 400$ GeV/c^2 for ee and $\mu\mu$ for all spins.

The primary and irreducible SM background results from Drell-Yan production of ee and $\mu\mu$ pairs. It is estimated using MC simulation normalized to fit to the data in the Z^0 peak, after the other background contributions have been subtracted. This reduces the effect of the luminosity uncertainty on the background estimate. The other contributions such as $t\bar{t}$ (generated with HERWIG [21]), $\tau^+\tau^-$, W^+W^-, and $W^\pm Z^0$ are estimated using MC simulation. Some accepted ee events come from non-dielectron sources, predominantly misidentified QCD dijet events. This background is estimated by extrapolating from events where the leptons are not isolated. The QCD background in the $\mu\mu$ channel is estimated using same-sign events that pass the selection criteria and is found to be small. The cosmic ray background in the $\mu\mu$ channel is estimated by applying the signal selection criteria to a sample of cosmic ray data collected by the CDF II detector and is non-negligible at high mass ($m_{\ell\ell} > 400$ GeV/c^2). Fig. 1 compares the estimated background distributions to the ee and $\mu\mu$ data. Table I shows the integrated number of events observed and expected above a given $m_{\ell\ell}$.

TABLE I: Integrated number of events above a given $m_{\ell\ell}$ for the observed data and estimated background.

$m_{\ell\ell}$	ee		$\mu\mu$	
(GeV/c^2)	Observed	Expected	Observed	Expected
> 150	205	212.9 ± 99.3	58	55.3 ± 2.5
> 200	84	78.2 ± 33.4	18	20.9 ± 1.0
> 300	22	13.6 ± 4.4	6	5.2 ± 0.3
> 400	5	2.9 ± 0.7	1	2.3 ± 0.2
> 500	2	0.8 ± 0.1	1	1.2 ± 0.1

Systematic uncertainties on the acceptance, efficiency and luminosity result in a relative uncertainty on the scale of $\sigma(X_{\ell\ell})$ of approximately 10%. The largest contributions are from the uncertainties on luminosity, energy/momentum scales and resolutions, and the choice of PDF as estimated by comparison of different PDF parameterizations. Background uncertainty in the ee channel ranging from 40-80% due to misidentified jets results in absolute uncertainties on values of $\sigma(X_{\ell\ell})$ that are large for $m_{\ell\ell} < 350$ GeV/c^2 but negligible at the higher mass region. Background uncertainties in the $\mu\mu$ channel are $\approx$ 30% and $\approx$ 20% due to fake muons and cosmic-rays respectively. The relative uncertainty with respect to the scale of $\sigma(X_{\ell\ell})$ on the electroweak backgrounds is $\approx$ 5% in the both channels.

Since no significant excess of events is observed, limits on $\sigma(X_{\ell\ell})$ are extracted using a Bayesian, binned likelihood method. For combined dilepton results assuming $BR(X \to ee) = BR(X \to \mu\mu)$, a joint likelihood is formed from the product of the individual-channel likelihoods accounting for the correlations among systematic uncertainties. When the nuisance parameters are integrated out, uncertainties on PDF, luminosity and common selection efficiencies are taken as 100% correlated among the different components of the acceptance. This joint likelihood is converted to a posterior density in the signal cross section and numerically integrated to obtain the 95% CL limits on $\sigma(X_{\ell\ell})$. Fig. 2 and Table II show the $\sigma(X_{\ell\ell})$ limits as a function of m_X with spins-0, 1, and 2. At high mass ($m_X > 600$ GeV/c^2) the limits are approximately 25 fb for all spins (but best for spin-0) and are consistent with expected limits in the absence of signal. The corresponding CDF Run I limit

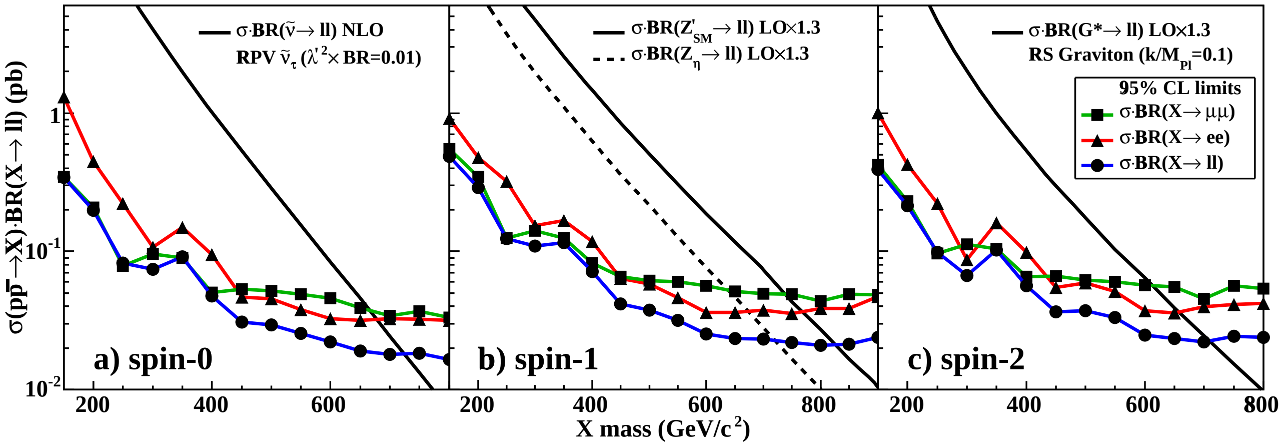

FIG. 2: The $\sigma(X_{\ell\ell})$ limits from ee, $\mu\mu$ and the combined channels as a function of m_X for spin-0 (a), spin-1 (b), and spin-2 (c). For the combined channel, $BR(X \to ee) = BR(X \to \mu\mu)$ ($\equiv BR(X \to \ell\ell)$) is assumed. Also shown are theoretical cross-section predictions of representative models.

TABLE II: 95% CL upper limits on $\sigma(p\bar{p} \to X) \cdot BR(X \to \ell\ell)$ (in fb) for a given m_X (in GeV/c^2). Spin-1 limits are computed to 900 GeV/c^2 to accommodate Z'models with large predicted cross-sections.

Spin\\m_X	150	200	250	300	350	400	450	500	550	600	650	700	750	800	850	900
Spin-0	340	200	83	74	91	48	31	29	26	22	19	18	18	17	—	—
Spin-1	490	290	120	110	120	72	42	38	32	25	24	23	22	21	21	24
Spin-2	390	210	98	67	100	56	37	37	33	25	24	22	24	24	—	—

was 40 fb [2]. The sensitivity of these searches is enhanced compared to the Run I searches by the addition of the plug-plug dielectrons (10% relative gain in ee acceptance), an increase in muon trigger coverage and the use of muons without muon-chamber tracks (50% relative gain in $\mu\mu$ acceptance). Fig. 2 also shows the predictions from representative models with higher order corrections [22]. The particle X is assumed to decay only to the known fermions in the mass range examined. From the spin-0 $\sigma(X_{\ell\ell})$ limit shown in Fig. 2(a), the lower mass bounds of 680, 620, and 460 GeV/c^2 from ee channel and 665, 590, and 450 GeV/c^2 from $\mu\mu$ channel are obtained for $\widetilde{\nu}$ for the coupling strength squared times branching fraction (λ'^2·Br)= 0.01, 0.005, and 0.001 respectively. For spin-1 (Fig. 2(b)) the following mass bounds are obtained from the combined channel: 825, 690, 675, 720 and 615 GeV/c^2 for $Z'_{\rm SM}$, Z_χ, Z_ψ, Z_η and Z_I respectively and 885, 860 ,805 and 725 GeV/c^2 for Z_H with the mixing parameter cot$\theta_H = 1.0$, 0.9, 0.7 and 0.5 respectively. Similarly, the lower mass limits of 280 GeV/c^2 (270 GeV/c^2) are set for ρ_{TC} and ω_{TC} in the TC model [9] with corresponding values of Technicolor-scale mass parameters $M_V = M_A$ of 500 GeV/c^2 (400 GeV/c^2). From the spin-2 $\sigma(X_{\ell\ell})$ limit shown in Fig. 2(c), the lower mass bounds of 710, 510, and 170 GeV/c^2 are obtained for the first excited state of the RS graviton for dimensionless coupling parameter ($k/M_{\rm PL}$) 0.1, 0.05, and 0.01 respectively, where k is the relative strength of the warped dimension's curvature scale and $M_{\rm PL}$ is the effective Planck scale. A method of factorizing the couplings, charges and $1/s$ dependence of Z' cross sections from kinematic factors that depend upon PDF parameterizations allows more general constraints on possible Z' models [6]. In this formalism, a generic Z' is described by two parameters, c_d and c_u, that define the coupling of down and up-type quarks to the resonance. Fig. 3 shows the bounds set by the spin-1 limits in the (c_d, c_u) plane along with the parameters describing the four E_6-model Z' bosons.

We thank D. Choudhury, A. Daleo, H. Logan, and S. Mrenna for their useful contributions. We thank the Fermilab staff and the technical staffs of the participating institutions for their vital contributions. This work was supported by the U.S. Department of Energy and National Science Foundation; the Italian Istituto Nazionale di Fisica Nucleare; the Ministry of Education, Culture, Sports, Science and Technology of Japan; the Natural Sciences and Engineering Research Council of Canada; the National Science Council of the Republic of China; the Swiss National Science Foundation; the A.P. Sloan Foundation; the Bundesministerium für Bildung und Forschung, Germany; the Korean Science and Engineering Foundation and the Korean Research Foundation; the Particle Physics and Astronomy Research Council and the Royal Society, UK; the Russian Foundation for Basic Research; the Comisión Interministerial de Ciencia y Tecnología, Spain; in part by the European

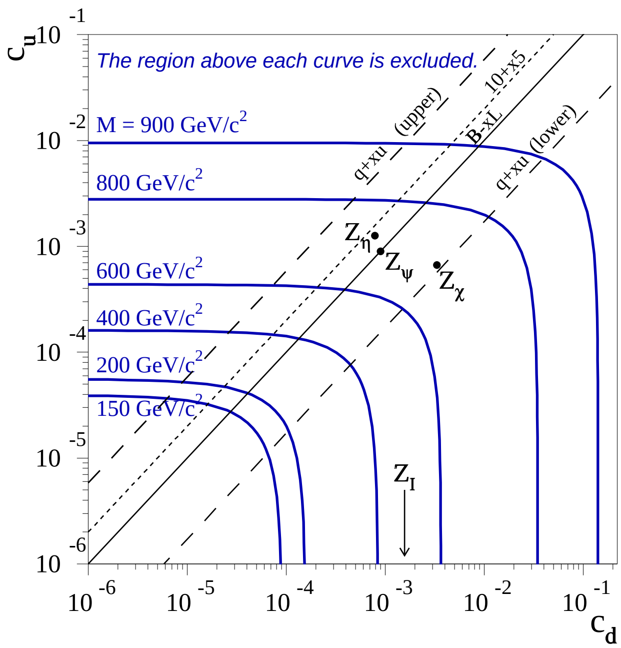

FIG. 3: Limit contours in the (c_d, c_u) plane [6] for a given Z' mass derived from the spin-1 $\sigma(X_{\ell\ell})$ limit. The solid and dotted diagonal lines show all possible models for the $U(1)_{B-xL}$ and $U(1)_{10+x\bar{5}}$ groups respectively. The two dashed lines show the range between which the values for the $U(1)_{q+xu}$ group must fall. The values for the $U(1)_{d-xu}$ group may fall anywhere on the plane. The parameters of the E_6-model Z' bosons are indicated.

Community's Human Potential Programme under contract HPRN-CT-2002-00292; and the Academy of Finland.

[1] M. Cvetic, D. A. Demir, J. R. Espinosa, L. L. Everett, and P. Langacker, Phys. Rev. **D56**, 2861 (1997), Erratum-ibid.**D58** 119905, (1998).
[2] CDF Collaboration, F. Abe *et al.*, Phys. Rev. Lett. **79**, 2192 (1997).
[3] D0 Collaboration, V.M. Abazov *et al.*, Phys. Rev. Lett. **87**, 061802 (2001).
[4] All the limits presented in this paper are at the 95% CL.
[5] LEP Collaboration, arXiv:hep-ex/0312023.
[6] M. Carena, A. Daleo, B. Dobrescu, and T. Tait, Phys. Rev. **D70**, 093009 (2004).
[7] F. del Aguila, M. Quiros, and F. Zwirner, Nucl. Phys. **B287**, 457 (1987).
[8] T. Han, H. E. Logan, B. McElrath, and L. Wang, Phys. Rev. **D67**, 095004 (2003), and H. E. Logan, private communication for PYTHIA implementation.
[9] K. D. Lane and S. Mrenna, Phys. Rev. **D67**, 115011, (1999).
[10] D. Choudhury, S. Majhi, and V. Ravindran, Nucl. Phys. **B660**, 343 (2003).
[11] L. Randall and R. Sundrum, Phys. Rev. Lett. **83**, 3370 (1999).
[12] CDF Collaboration, D. Acosta *et al.*, Phys. Rev. **D71**, 032001 (2005).
[13] CDF uses a cylindrical coordinate system in which ϕ is the azimuthal angle, and $+z$ points in the direction of the proton beam and is zero at the center of the detector. The pseudorapidity $\eta \equiv -\ln(\tan(\theta/2))$, where θ is the polar angle relative to the z axis. Calorimeter energy (track momentum) measured transverse to the beam is denoted as $E_{\rm T}$ ($p_{\rm T}$), and the total calorimeteric transverse energy imbalance is denoted as $\not{E}_T$.
[14] CDF Collaboration, D. Acosta *et al.*, Phys. Rev. Lett. **94**, 091803 (2005).
[15] CDF Collaboration, D. Acosta *et al.*, Phys. Rev. **D71**, 051104 (2005).
[16] A. Kotwal *et al.*, Nucl. Instrum. Meth. **A506**, 110 (2003).
[17] K. Ikado, Ph.D. thesis, Waseda University, **3809** (2004), FERMILAB-THESIS-2004-61.
[18] M. Karagöz Ünel, Ph.D. thesis, Northwestern University, Diss 378 NU 2004 K18s, FERMILAB-THESIS-2004-47.
[19] T. Sjöstrand *et al.*, Computer Phys. Commun. **135**, (2001).
[20] H. L. Lai *et al.*, Eur. Phys. J. **C12** 375 (2000).
[21] G. Corcella *et al.*, JHEP **01**, 10 (2001).
[22] A constant K-factor of 1.3 is used to be consistent with the previous analyses making comparison of the Z'mass limits easier. The NLO calculation is used for the RPV $\tilde{\nu}$ case. The dependence on the higher order corrections for the $\sigma(X_{\ell\ell})$ limits is negligible.